Infiltration of Electrolytes in Molecular-Sized Nanopores

Ling Liu and Xi Chen
School of Engineering and Applied Sciences, MC 4709, Columbia University, New York, New York 10027, USA

Weiyi Lu, Aijie Han, and Yu Qiao*
Department of Structural Engineering, University of California—San Diego, La Jolla, California 92093-0085, USA
(Received 26 December 2008; published 6 May 2009)

In both experiment and molecular simulation, it is found that a higher pressure is required to sustain the infiltration of smaller ions in a molecular-sized nanochannel. Simulations indicate that the effective ion solubility of the infiltrated liquid is reduced to nearly zero. Because of the strong interactions between the ion couples and the solid or liquid phases, an external force is required to continuously advance the confined liquid segment. The competition between the probability of ion entry and ion-couple formation causes the observed ion-size-dependent characteristics.

DOI: 10.1103/PhysRevLett.102.184501 PACS numbers: 47.61.−k, 47.60.Dx, 47.61.Cb

Understanding ion behavior in a nanochannel has drawn increasing attention [1,2], due to its fundamental role in a number of emerging areas including selective ion conduction, absorption and adsorption, sensing, energy conversion and storage, etc. [3–5] In bulk water, a molecular cluster can be formed around a solvated ion [6]. As the ions transport inside a nanotube of a diameter comparable with the characteristic size of the molecular cluster, the solvated configuration can be distorted [7]. Insights into the molecular configurations can be sought from first principle and molecular dynamics (MD) studies [8–12].

In a small nanotube or nanochannel, liquid molecules and ions can form a quasi-one-dimensional chain [12–17]. If the nanotube or nanochannel surface is effectively nonwettable, an external driving force must be applied to force the ions and liquid molecules to enter the nanoenvironment [18–20]. That is, work must be done to increase the system free energy. It is envisioned that, for solvated ions of the same ion charge but different ion sizes, the required external force would be specific [21], depending on the variation in system free energy. It was generally predicted that for the same nanopore, if the solvent molecular or ionic size increases, less pore volume is available and the infiltration pressure should be higher. Even when the nanochannel wall is nominally wettable in the liquid phase, the channel size must be much larger than the solute molecules or ions; otherwise the repelling effect of the solid wall would prevent their infiltration. The required ''free volume'' can be a few times larger than the solvent molecules or ions [22,23]. This prediction, however, may break down for a very small nanochannel where the effective channel diameter is only slightly larger than the ion size. In this case, ions can directly interact with the channel wall, which not only affects the solid-liquid interaction but also dominates the configuration of the confined clusters of electrolyte particles.

To explore the unique transport behaviors of an electrolyte in molecular-sized nanochannels, we investigated a zeolite Y, ZY. Compared with many other nanoporous materials, zeolites are of highly ordered porous structures. The ZY sample has an effective pore diameter of 0.7 nm [24]; it was placed in a steel cylinder with an aqueous solution of chloride salt, with the ZY-to-liquid mass ratio of 1/10. The salt was either LiCl, NaCl, KCl, or CsCl, and the molarity of all the solutions was $4M$. (More experimental details are given in the supplementary material [25].)

The ZY material was effectively hydrophilic. Therefore, if the liquid phase was pure water, the nanopores could be soaked up spontaneously; if an external pressure was applied, the compression behavior was quite linear, determined by the machine compliance and the liquid bulk modulus. As the electrolyte was added, the nanopore inner surface might become effectively nonwettable [26], and under ambient pressure the nanopores remained empty. As an sufficiently high external pressure was applied, pressure-induced liquid infiltration began, leading to the formation of an infiltration plateau in the sorption isotherm curve (Fig. 1). The liquid infiltration ended when the porous space was filled up. The width of the infiltration plateau reflected the accessible nanopore volume, close to the measured porosity, as it should be. The measurement results of the infiltration pressure, p_{in}, are also shown in Fig. 1. For self-comparison purpose, p_{in} was taken as the pressure at the starting point where the measured slope of the sorption isotherm curve is a constant afterwards.

It is remarkable that p_{in} decreased with the cation size. For the LiCl solution, p_{in} was nearly 15 MPa; when the electrolyte was changed to NaCl, p_{in} became 13.5 MPa; for KCl, p_{in} was largely decreased to 4 MPa. In the pure water and the CsCl based systems, the pressure-induced infiltration could not be detected, indicating that the nominal p_{in} was zero; i.e., the nanopores could be filled by the liquid phase spontaneously at ambient pressure.

In order to understand the unique ion behaviors, atomistic simulations and energy analyses are carried out and

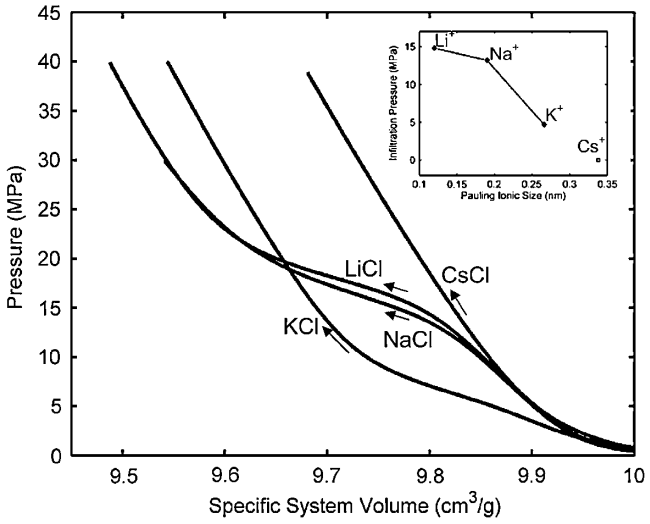

FIG. 1. Typical quasistatic sorption isotherm curves. The insert at the upper-right corner shows the infiltration pressure as a function of the Pauling cation size. The specific system volume is defined as the system volume normalized by the mass of the nanoporous material. The arrows indicate the loading direction.

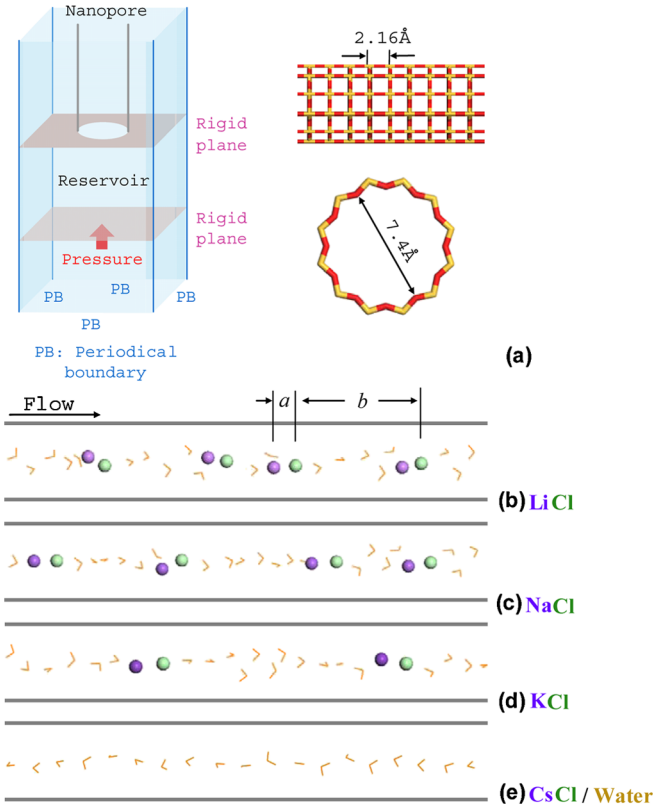

FIG. 2 (color online). The MD simulation: (a) schematic of the infiltration process and a model SiO_2 nanochannel that mimics a single nanopore of zeolite Y. Snapshots of the pressure-driven infiltrated ion or water structures of (b) LiCl, (c) NaCl, and (d) KCl electrolytes, inside the nanochannel and upon steady-state. Each Cl^- [light gray (green) ball] is followed by a cation [dark gray (purple) ball], forming a number of anion-cation couples with water molecules in between. The ion couple sizes and the distances between adjacent ion couples of different infiltrated electrolytes are significantly different. (e) In the CsCl solution, only H_2O molecules can infiltrate into the nanopore.

elaborated on below. We performed a MD simulation where a long, straight, and rigid silicon dioxide nanotube [Fig. 2(a)] with the diameter of $D_0 = 7.4$ Å (the distance between diagonal O atoms) was employed as a close analog to a ZY nanopore. The model setup was similar to that in experiment (more details are given in the materials and methods section in the supplementary material [25]). To be consistent with the experiment, ions and water molecules were mixed uniformly in the reservoir with the molarity of $4M$. Upon increase of the reservoir pressure, p, the water molecules and ions inside the reservoir-nanochannel system were redistributed, and at a critical pressure (p_{in}), they may continuously enter the nanochannel, reflecting the adiabatic pressure-driven electrolyte transport in a nanopore.

The simulation results show that for three of the electrolyte solutions under investigation, LiCl, NaCl, and KCl, only at an elevated pressure level can ions and water molecules infiltrate into the nanochannel. The value of p_{in} is the highest for LiCl and the lowest for KCl. For the CsCl solution that is of the largest cation size, water molecules enter the channel at ambient pressure whereas no ion infiltration can be observed even at $p > 100$ MPa; i.e., the nominal p_{in} of CsCl solution is zero. These observations are in agreement with the experimental results.

Owing to the strong confinement effect of the nanochannel, the infiltrated water molecules and ions maintain a quasi-one-dimensional chain, as shown in the snapshots from MD simulations, Figs. 2(b)–2(e). It is remarkable that the distribution of ions is highly regular at the steady-state: each Cl^- ion couples with a cation (Li^+, Na^+, or K^+), forming a number of anion-cation couples with ordered sequence, and the ion couples are separated by a few water molecules. It is also noteworthy that in the nanotube under investigation, the ion infiltration process in Figs. 2(b)–2(d) is always led by a cation in the flow direction and followed by the quasiperiodical anion-cation couples, and thus the electrolyte segment inside the nanopore is typically non-neutral. Such commonality of ion infiltration sequences (shared by the three electrolytes that can infiltrate into the nanochannel) can be explained via an energy analysis (section 1 of the supplementary material [25]). Compared with the uniformly scattered ion distribution in bulk liquid phase, the current atomistic simulation suggests that in a highly confined space, there is an energetic preference for a cation and anion to form a nanocrystallinelike structure (section 3 of the supplementary material [25]). That is, as the space is insufficient for any solvated structure, the effective solubility of ions is greatly reduced.

The ion-couple size, i.e., the averaged spacing between the two ions in a couple (a), and the averaged distance

between adjacent ion couples (b), are different for different electrolytes [Figs. 2(b)–2(d)]: MD simulations show that the larger the cation, the larger a and b—such unique characteristics of the confined ion structure are responsible for the observed ion-size effect on the infiltration pressure, p_{in}. In particular, the value of a is dominated by the equilibrium of Coulomb attraction and van der Waals repulsion in an anion-cation couple. For Li^+-Cl^-, Na^+-Cl^-, and K^+-Cl^- ion couples, an independent energy calculation shows that the equilibrium distance is 2.05 Å, 2.39 Å, and 2.74 Å, respectively, which is close to the average values of a identified from the MD simulation snapshots: 2.20 Å, 2.55 Å, and 2.8 Å, respectively. The small difference between them can be attributed to the environmental factors, e.g., the presence of the nanochannel wall and the water molecules. Compared with a, the ion-size dependence of b is of more interest, which implies a better chance for a smaller cation to enter the nanochannel that can be validated by an independent energy barrier analysis (section 2 of the supplementary material [25]). The results show that small cations have the advantage during the competition for infiltration with water molecules, leading to a higher frequency of ion infiltration and thereby a smaller separation distance between the ion couples (i.e., a smaller b).

Immediately after the infiltration of a cation (Li^+, Na^+, or K^+), either an anion (Cl^-) or a water molecule may enter the nanotube. It is possible that near the nanochannel opening, an infiltrated cation and an anion may be separated by a few water molecules. However, since both the cation and anion cannot be fully solvated in the small nanochannel, aided by the long-range electrostatic attraction, the two ions can "aggregate" inside the tube, forming an ion couple. According to the energy analysis elaborated on in section 3 of the supplementary material[25], the aggregation of two oppositely charged ions favorably reduces the system potential, and the resulting nanocrystallinelike structure is highly stable [27].

These structural features and size-dependent variables of the infiltrated ion or molecule structure dominate the infiltration pressure, p_{in} [28,29]. When the size of nanochannel is fixed, p_{in} is governed by the effective solid-liquid interfacial tension, $\Delta\gamma$. A possible contribution to $\Delta\gamma$ arises from the difference between the free energies of the same liquid volume in bulk and confined states, denoted as $\Delta\gamma_0$. Energy analyses show that $\Delta\gamma_0$ of water, LiCl, NaCl, and KCl solutions are all small negative values, indicating that, without considering other factors, all of them should be able to spontaneously enter the tube at ambient pressure.

In the MD simulation and the experiment, however, such spontaneous infiltration is observed only with pure water and the CsCl solution. Because of the polarity of ion couples and the non-neutrality of infiltrated liquids, $\Delta\gamma$ is also dependent on the requirement of sustaining the ion transport after infiltration. As remarked earlier, when the ions and water molecules enter the nanochannel as a quasiperiodical chain, with the cation leading the infiltrated segment, the remaining electrolyte in the reservoir is non-neutral, and a negative charge is needed to effectively balance the confined charges. Since the cation in any infiltrated ion couple is closer than the anion to the effective negative charge outside the nanopore [Figs. 2(b)–2(d)], a strong net Coulomb attraction is yielded, causing an additional energy barrier, $\Delta\gamma'$. That is, $\Delta\gamma = \Delta\gamma_0 + \Delta\gamma'$. The value of $\Delta\gamma'$ can be assessed as the energy consumption by each ion couple, ΔE, multiplied by the number of ion couples per unit area of the infiltrated segment, n. Both of the variables are ion-size dependent, where ΔE is affected by a and n is influenced by b.

An energy analysis is carried out to estimate ΔE. Figure 3 plots the energy variations. Note that the second derivatives of these curves are negative, suggesting that the work required for transporting ions becomes less as the ion couple is moved farther away from the tube opening, due to the decrease in Coulomb interaction. As the ion couples have traveled for about 500 Å, the energy variations become quite slow. From Fig. 3, the K^+-Cl^- couple has the largest energy barrier, approximately 0.55 kCal/mol, followed by the Na^+-Cl^- couple with 0.53 kCal/mol, and the ΔE of Li^+-Cl^- is about 0.45 kCal/mol. Such variation is primarily due to the difference in a. With a smaller a value, the anion in the Li^+-Cl^- couple can offset more attraction between the Li^+ and the effective charge outside the nanopore, leading to a smaller net force.

The associated free energy change of the steady-state system is $\Delta\gamma' = \frac{\Delta E}{\pi b D}$, where D is the effective diameter of the liquid segment [29]. The difference of quasistatic pressure (before and after infiltration) should be balanced by

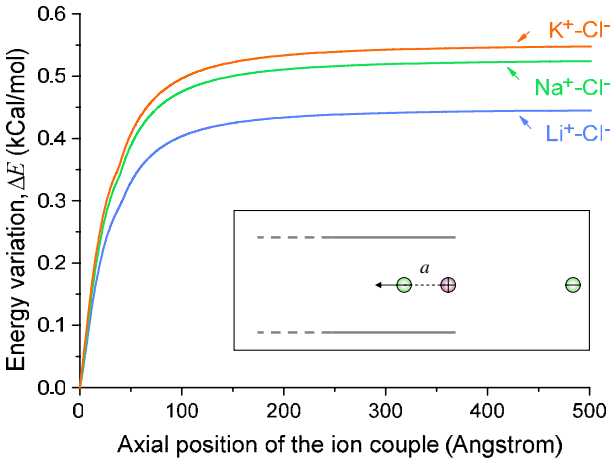

FIG. 3 (color online). Energy analysis when an anion-cation couple (with an equilibrium separation, a) is moved toward the interior of the nanopore; the net interaction energy with the system is plotted as a function of the ion couple's axial travel distance (from the pore opening).

the system free energy increase, i.e., $p_{in} = 4\Delta\gamma/D$. Since $\Delta\gamma_0$ is negligible for the investigated cases, p_{in} is nearly proportional to ΔE and $1/b$. Although the KCl solution has the largest ΔE, its p_{in} is still calculated to be the lowest, 8.85 MPa, due to the large separation distance between ion couples, b. The NaCl and LiCl solutions have the p_{in} values of 14.64 MPa and 15.69 MPa, respectively. Using this model, the predicted ranking and values of p_{in} agree quite well with the data of the experiment and the MD simulation [30].

To summarize, we report an interesting phenomenon that, when other conditions remain the same, it requires a higher pressure to sustain the infiltration of an electrolyte solution of a smaller cation size into a molecular-sized nanochannel. The MD simulation indicates that the confined ions tend to form crystallinelike ion couples; i.e., a quasi-one-dimensional water molecular chain cannot dissolve any ions (nor any gas molecules [31]). There is a strong sequence preference of the ions entering the nanopore, forming a non-neutral, quasiperiodical structure. Ions of smaller sizes have a higher probability to infiltrate into the nanochannel, and thus the spacing between ion couples is smaller. In order to sustain continuous transport, an external work must be applied on the system, such that the infiltrated liquid segment could overcome the energy barrier imposed by the nonbonded interaction with the rest of the system. For smaller ions, although it requires less work to advance a unit ion couple, the spacing between ion couples is more dominant to the required work, which leads to a higher infiltration pressure.

The work was supported by the NSF and the Sandia National Lab under Grant No. CMMI-0623973, and the NSF under Grant No. CMMI-0643726. L. L. acknowledges the support of the American Academy of Mechanics and the Robert M. and Mary Haythornthwaite Foundation.

*Corresponding author.
yqiao@ucsd.edu

[1] R. B. Schoch, J. Y. Han, and P. Renaud, Rev. Mod. Phys. **80**, 839 (2008).
[2] A. Holtzel and U. Tallarek, J. Sep. Sci. **30**, 1398 (2007).
[3] S. Guenes and N. S. Sariciftci, Inorg. Chim. Acta **361**, 581 (2008).
[4] K. Healy, B. Schiedt, and A. P. Morrison, Nanomedicine **2**, 875 (2007).
[5] W. Lu *et al.*, Appl. Phys. Lett. **94**, 023 106 (2009).
[6] C. H. Hamann, A. Hamnett, and W. Vielstich, *Electrochemistry* (Wiley-VCH, New York, 2007).
[7] S. Joseph *et al.*, Nano Lett. **3**, 1399 (2003).
[8] M. Khazaei *et al.*, J. Phys. Chem. B **108**, 15 529 (2004).
[9] Q. Shao *et al.*, Phys. Chem. Chem. Phys. **10**, 1896 (2008).
[10] L. Yang and S. Garde, J. Chem. Phys. **126**, 084 706 (2007).
[11] M. Carrillo-Tripp, H. Saint-Martin, and I. Ortega-Blake, Phys. Rev. Lett. **93**, 168104 (2004).
[12] G. Hummer, J. C. Rasaiah, and J. P. Noworyta, Nature (London) **414**, 188 (2001).
[13] M. Majumder *et al.*, Nature (London) **438**, 44 (2005).
[14] K. Y. Chan, Y. W. A. Tang, and I. Szalai, Mol. Simul. **30**, 81 (2004).
[15] S. Joseph and N. R. Aluru, Nano Lett. **8**, 452 (2008).
[16] H. Daiguji, P. Yang, and A. Majumdar, Nano Lett. **4**, 137 (2004).
[17] Y. W. Tang, K. Y. Chan, and I. Szalai, Nano Lett. **3**, 217 (2003).
[18] A. Han and Y. Qiao, J. Mater. Res. **22**, 644 (2007).
[19] X. Kong and Y. Qiao, Appl. Phys. Lett. **86**, 151 919 (2005).
[20] X. Kong and Y. Qiao, J. Appl. Phys. **99**, 064 313 (2006).
[21] F. Fornasiero *et al.*, Proc. Natl. Acad. Sci. U.S.A. **105**, 17 250 (2008).
[22] D. T. Wasan and A. D. Nikolov, Nature (London) **423**, 156 (2003).
[23] A. Han and Y. Qiao, J. Am. Chem. Soc. **128**, 10 348 (2006).
[24] S. M. Auerbach, K. A. Carrado, and P. K. Dutta, *Handbook of Zeolite Science and Technology* (CRC Press, Boca Raton, FL, 2003).
[25] See EPAPS Document No. E-PRLTAO-102-040920 for supplementary material. For more information on EPAPS, see http://www.aip.org/pubservs/epaps.html.
[26] A. Han and Y. Qiao, Appl. Phys. Lett. **91**, 173 123 (2007).
[27] Although the current simulations are specified for a polar zeolite nanopore, we note that even if the nanopore is nonpolar (e.g., a carbon nanotube), small cations are still favored to infiltrate the nanochannel, and each cation would attract an anion, forming a similar quasiperiodical structure (although the infiltrated segment would be neutral).
[28] The infiltration pressure refers to the pressure at the critical moment, after the transport of the liquid segment inside a nanopore reaches steady-state. Before such a critical point, the system free energy variation associated with infiltration is not a constant, leading to nonlinear variations in the required pressure. During steady-state transport, the pressure varies linearly with the infiltration volume.
[29] Y. Qiao, L. Liu, and X. Chen, Nano Lett. 9, 984 (2009).
[30] Similar cation-size-dependent infiltration behavior is also observed if the nanochannel is nonpolar, where the van der Waals interaction dominates the interaction between the infiltrated quasiperiodical ion structure and solid wall. Such interaction is weaker compared to the electrostatic forces in a polar nanochannel, and thus the ion-size effect is less prominent.
[31] Y. Qiao, G. Cao, and X. Chen, J. Am. Chem. Soc. **129**, 2355 (2007).

MATERIALS AND METHODS

Experimental: The as-received material was provided by Zeolyst (Part No.: CBV-901) in powder form, with the crystal size of 10-50 μm and the porosity of about 0.2 cm^3/g. The relatively large crystal size assured that the ion transport could reach the steady state under a quasi-equilibrium loading. In order to minimize the defect density at nanopore inner surfaces, the ZY crystals were first thermal treated in air at 175 ºC for 6 h and then placed in a vertical quartz tube furnace. A nitrogen flow was conducted across the tube furnace, carrying saturated silicon tetrachloride vapor through the sample. The temperature was kept at 400 ºC for 1 h, after which the ZY sample was cooled in air and thoroughly washed by distilled water, and then heated at 500 ºC in air for 1.5 h and dried in vacuum at 50 ºC for 8 h. During the infiltration experiment, the zeolite-liquid mixture was sealed in a stainless steel cylinder by a stainless steel piston. The piston was intruded into the cylinder at the rate of 0.5 mm/min by a type 5580 Instron machine, until the inner pressure reached 40 MPa. Further reducing loading rate would not cause any detectable change in sorption isotherm curve, indicating that such a loading condition could be regarded as quasi-static. The system volume change was calculated as $A_p \cdot d_p$, where A_p = 286 mm^2 is the cross-sectional area of the piston and d_p is the piston displacement. The inner pressure was calculated as F_p/A_p, where F_p is the intrusion force applied on the piston, measured by a 100KN loadcell.

Numerical: The MD simulations are performed with the COMPASS force field (H. Sun, J. Phys. Chem. B 102, 7338 (1998)). During simulation, one end of the nanochannel was immersed in a 20Å×20Å×100Å liquid reservoir. The liquid in the reservoir was bounded by two rigid planes (walls) in the axial direction, and periodical boundary condition was imposed in the transverse directions (Fig. 2a). The anion was chlorine (Cl^-), and the cation was lithium (Li^+), sodium (Na^+), potassium (K^+), or cesium (Cs^+). The cations were of the same ionic charge and their Pauling ionic radii were 60, 95, 133, 169 pm, respectively. After initial optimization of 100 ps at the pressure of 1 atm and the temperature of 300K, the ions were evenly solvated among the water molecules in the reservoir. The reservoir pressure can be raised by reducing its volume along axial direction (Fig. 2a). All simulations are carried out sufficiently slow such that the process can be regarded as nearly quasi-static pressure-induced infiltration. The MD simulation also confirms that for pure water, the nanochannel is hydrophilic and the water molecules would enter the nanopore under ambient conditions, which is consistent with the experimental result that p_{in}=0 for pure water.

SUPPLEMENTAL RESULTS

In the three sections below, based on energy analyses and physics based models we respectively answer the following key questions: Why do the infiltrated ions form an ordered sequence shown in Fig.2 (i.e. a cation followed by a number of anion-cation couples)? How does the nanocrystalline-like ion couple form inside the molecular-sized channel where the effective solubility of ions is essentially zero? Why does the spacing between adjacent ion couples depend on the cation size?

1. Mechanism of the formation of the ordered sequence of infiltrated ions

An independent energy analysis is performed to shed light on the ordered sequence of ions (Fig.2b-e) found in the MD simulation, which is a commonality among the three ion infiltration cases (LiCl, NaCl, and KCl). Starting from an empty nanotube, we compare the energy barriers of the infiltration of an anion and that of a cation. It is assumed that all ions are centrally located and moved along the axial direction. After an ion enters the tube, the process is repeated to identify the next preferred one. Eventually, a sequence of the ion distribution can be determined.

Three key instants are examined, as shown in Fig.S1(a). Stage 1 refers to the instant when the *first* ion is infiltrated, where "1A" illustrates the possibility that a cation (positioned at the tube opening) would infiltrate the nanopore, and "1B" corresponds to the alternative situation that an anion would first enter the same nanotube. In either case, there is a counter-charge placed outside the tube to keep the system neutral. The position of the counter-charge is determined such that it could reproduce the same force acting on the infiltrated ions as that imposed by the electrolyte solution outside the nanopore in the MD simulation. The examined ion is then perturbed by several Å along the axial direction, and its interaction energy with the nanotube and the counter-charge is computed. The energy variations are plotted in Fig.S1(b), where an upwards curve implies energy consumption while the downward trend indicates an energetically favorable process. It is clear that from the energy point of view, it is preferred for a cation to first enter the nanopore prior to an anion, since in the examined nanochannel the influence of the oxygen atoms is more pronounced. The subsequent stage 2 assumes that a cation has already infiltrated, and we explore which ion (a cation or an anion) tends to infiltrate next. In this case, the counter-charge should be -2e for case "2A" and 0 for case "2B". As plotted in Fig.S1(c), configuration "2A" decreases system energy and therefore another cation can enter the nanopore (primarily owing to the size of the small cation). Similarly, the analysis of stage 3 (Fig.S1d) indicates that an anion tends to follow the two previously infiltrated cations.

The above analyses reveal that the sequence of the first three infiltrated ions should be cation → cation → anion, as illustrated in Fig.S2 (stages 1~3), which holds for all the three electrolytes under investigation: LiCl, NaCl, and KCl (Cs^+ cannot infiltrate the nanochannel, which will be discussed in the next section). Note that, the opposite ions (e.g. the 2nd and 3rd ions) in the nanochannel tend to approach and pair with each other because of the Coulomb attraction – the formation mechanism of such ion couple is discussed in Sect.3 of the Supplement.

After the infiltration of the first three ions (stage 4), there is only one net positive ion charge inside the channel and one counter-charge outside, leading to a situation similar to the end of stage 1 in Fig.S2. Thus, the subsequent infiltration of ions would repeat stages 2~4, as more and more cation-anion couples enter the nanochannel (stage 5). Once the ion couples are deep

inside the tube, due to the interaction with the leading cation, the anion and cation would prefer to switch their positions to reduce energy (stage 5). Finally, a quasi-periodical chain-like structure of infiltrated ions is formed (stage 6 in Fig.S2, the "steady-state"): almost all the infiltrated ions form couples, led by an anion closely followed by a cation, except that in the infiltration front there is a single cation, and at the end of the chain (at the tube opening) the ion couple just infiltrated is led by a cation followed by an anion. Due to the hydrophilic nature of the tube under investigation, a few water molecules may separate the infiltrated ion pairs. Such configuration predicted from energy analysis matches qualitatively with the sequence of the infiltrated ions in MD simulation (Fig.2).

2. Size dependent geometry of the quasi-periodical structure of infiltrated ions

The analysis in Sect.1 shows that it is energetically favorable for cations and anions to enter the nanochannel with a regular pattern. However, such similarity of infiltration sequence (shared by LiCl, NaCl, and KCl) cannot explain the intriguing ion size effect on the ion transport pressure, p_{in}, for which the details of the ion structure must be examined.

Figure 2 shows that the averaged spacing between ion couples, b, is smaller for smaller cations, suggesting that the possibility of infiltration of a smaller cation is higher. The results in Fig.S1(b-d) are computed by moving respective ions along the axial direction, where there is not much difference among Li^+, Na^+, and K^+. Recall that during the actual infiltration process in the MD simulation, the in-plane motion of ions is important due to the thermal vibration and the complex multi-body interactions. Thus, a refined energy analysis is performed.

In Fig.S3, an in-plane energy analysis is carried out, where an energy contour plot is established by moving an cation or a water molecule in the cross section of the channel. For a water molecule, the orientations of H-O bonds are optimized during this process. For small ions such as Li^+ and Na^+ ions, a large plateau is found in the central part of the channel, within which the energy is only slightly varied – at any point inside this region, the ion has nearly the same probability of infiltration. By contrast, the energy plateau is small (i.e. the radial gradient of energy is quite high) for large cations such as Cs^+, mainly due to their large vdW radii.

Considering cations at the tube opening, a smaller one (e.g. Li^+ or Na^+) has a larger potential entry area within which the energy barrier is low, and thus statistically, the probability of infiltration is higher. This gives a smaller cation more advantage in its competition of infiltration with water molecules, leading to a higher frequency of ion infiltration and thereby a smaller b (compared with larger ions). When the cation is too large, such as for Cs^+, the infiltration is energetically unfavorable, and this explains why only water molecules could enter the hydrophilic nanopore and ions are left outside in the CsCl solution.

When the nanopore is neutral (e.g. a carbon nanotube, CNT), a similar energy analysis shows that the small cation is still preferred to infiltrate the nanotube, and followed by an anion. A similar periodical structure would still form in the sequence of cation-anion couples, although the overall infiltrated structure is typically neutral.

3. Mechanism of the formation of nanocrystalline-like ion couples

The energy analyses above show that after the infiltration of a cation, either an anion (Cl^-) or a water molecule may enter the tube with similar probabilities. It is possible that close to the tube opening, an infiltrated cation and an infiltrated anion are separated by a few water

molecules. However, upon steady-state, one of the interesting features of the infiltrated ion structure is the formation of nanocrystalline-like ion couples, which indicates that the solvation of ions is essentially impossible in a molecular-sized nanochannel. In other words, once well inside the nanotube, the infiltrated ions are no longer scattered; instead, a cation always approaches and pairs a nearby anion, until all water molecules initially bounded by the two ions, if any, are "pushed away" from the cation side, thus forming an ion couple.

In order to understand this procedure from an energy perspective, two factors need to be taken into account. One is the variation of system free energy associated with the transition from a scattered ion structure (Fig.S4a) to a paired ion structure (ion couples, Fig.S4b), and the other is the energy barrier for water molecules to bypass the ions embracing them.

Taking the infiltrated NaCl electrolyte as an illustrative example, we first estimate the energy variation induced by the structural change. The ion structure is assumed to have parameters approximately equal to those obtained from the MD simulation: in the nanocrystalline-like (paired) structure (Fig.S4b), the spacing between the two ions in a couple is a=2.4Å and the separation between adjacent ion couples is b=15Å, both consistent with Fig.2(c); in the scattered ion structure (Fig.S4a), we assume all ions are separated with an identical spacing of c=8.7Å. Due to the prominent electrostatic interactions among ions, the influence of water molecules is secondary. The potential energy of the two ion structures are evaluated as -751kCal/mol and -299kCal/mol, respectively, implying that the formation of ion couple is accompanied by a prominent energy reduction of about 75 kCal/mol, which is therefore energetically favorable.

For the scattered state (Fig.S4a) to become the nanocrystalline-like structure (Fig.S4b), an energy barrier must be overcome: when the two oppositely charged ions approach each other, water molecules in between them, if any, must escape the encirclement by bypassing an ion (Fig.S4d). During this process, the energy barrier peaks when a water molecule and an ion are within the same cross-section (when they are about to switch their positions). By minimizing the potential energy with respect to the in-plane positions of a water molecule and an ion (Fig.S4e), the energy barrier is evaluated to be 5kCal/mol for a water molecule to bypass a Na^+ and 64kCal/mol to bypass a Cl^-. Apparently, the larger size of Cl^- leads to a higher energy barrier and the water molecule prefers to switch position with the Na^+.

Comparing 75kCal/mol and 5kCal/mol, energetically, the energy reduction associated with structural reorganization is much larger than the energy barrier. Consequently, the oppositely charged ions would have a strong intention to approach each other, at the expense for bounded water molecules to switch their positions with a cation, such that the ion couple can be formed eventually. If the separation between the two ions is too large, such ion couple may be difficult to form. Such a pathway matches with ob[1]servations in the MD simulation very well.

Given that the above structural change is irreversible, in order to keep the nanocrystalline-like structure (Fig.S4b) stable (such stability was observed in the MD simulation, Fig.2b-d), the formed ion couple configuration (Fig.S4b) should not further aggregate to a continuous ion strand (Fig.S4c). Another energy analysis is carried out, where the potential energy of the nanocrystalline-like (Fig.S4b) and the aggregated (Fig.S4c) structures are calculated as -751kCal/mol and -937kCal/mol, respectively. Theoretically, the structural reorganization from Fig.S4(b) to Fig.S4(c) would possess an energy reduction of 44kCal/mol. However, a prerequisite for the formation of such an aggregated structure (Fig.S4c) is that the bounded water molecules must be able to bypass the large Cl^- ion, which has an energy barrier as high as 64kCal/mol, larger than the overall potential gain. Thus, aggregation of nanocrystalline-

like ion couples is not likely to occur. From energy point of view, a larger nanocrystalline-like structure would only form when two ion couples entered the nanopore one after another, such as a Na+ immediately followed by a Cl-, a Na+, and another Cl- without any water molecules in between them. This is theoretically possible but the probability is quite small, and was never observed in our MD simulation.

All these energy analyses match the MD simulation quite well: once an anion and a cation are both inside the nanopore, they approach and pair each other while water molecules in between are "pushed away" from the cation side. Following this procedure, nanocrystalline like ion couples are formed for all the three infiltrated electrolytes (Fig.2b-d). The structure of ion couples thus formed is quite stable. Energetically, the formation of ion couples is irreversible. Similar formation mechanism of ion couples also holds in a neutral molecular-sized nanochannel (e.g. a carbon nanotube).

It should be noted that in order for the ion-couples mechanism to become prominent, two preconditions are required:

(i) The nanochannel size must be molecular sized; i.e. at the level of a few Å. Only under this condition can the hydration of ions be severely distorted, making two oppositely charged ions more inclined to aggregate and form a nanocrystalline-like structure.

(ii) The study should focus on the transient process of ion transport from a bulk reservoir into the nanochannel. The dynamic transition from bulk state to confined state can greatly assist the formation of ion couples, as established equilibrium (fully developed hydration shells) is destructed and ions are seeking for new equilibrium inside the channel.

FIGURE CAPTIONS

Figure S1. Energy analysis of the axial motion of individual ions: (a) the six cases examined, each corresponding to a possible ion infiltration sequence at a representative instant during the infiltration process; in each case, the ion at the tube opening is perturbed by 1.5Å ~3Å along the tube axis; (b)-(d) the interaction energy between the moving ion and the system, where the possibility "A" is more energetically favorable at all instants.

Figure S2. Step-by-step schematic of the sequential infiltration and configuration of ions inside the nanochannel (water molecules are not shown).

Figure S3. Energy analysis of the in-plane motion of individual ions and water molecule: the ion/molecule is placed at various positions around the tube center to measure the variation of its interaction energy with the nanopore. The energy value at the tube center is adopted as the ground state. The diameter of the black circle equals to 4.5Å.

Figure S4. Energy analysis of the formation of nano-crystal-like ion couples: (a) postulated scattered ion structure; (b) paired ion structure (the nano-crystalline-like ion couples observed in MD simulations, Fig.2); (c) a postulated continuous ion strand; (d) an cation approaches a nearby anion by pushing away water molecules in between; (e) the instant when a cation bypasses a water molecule.

Figure S1

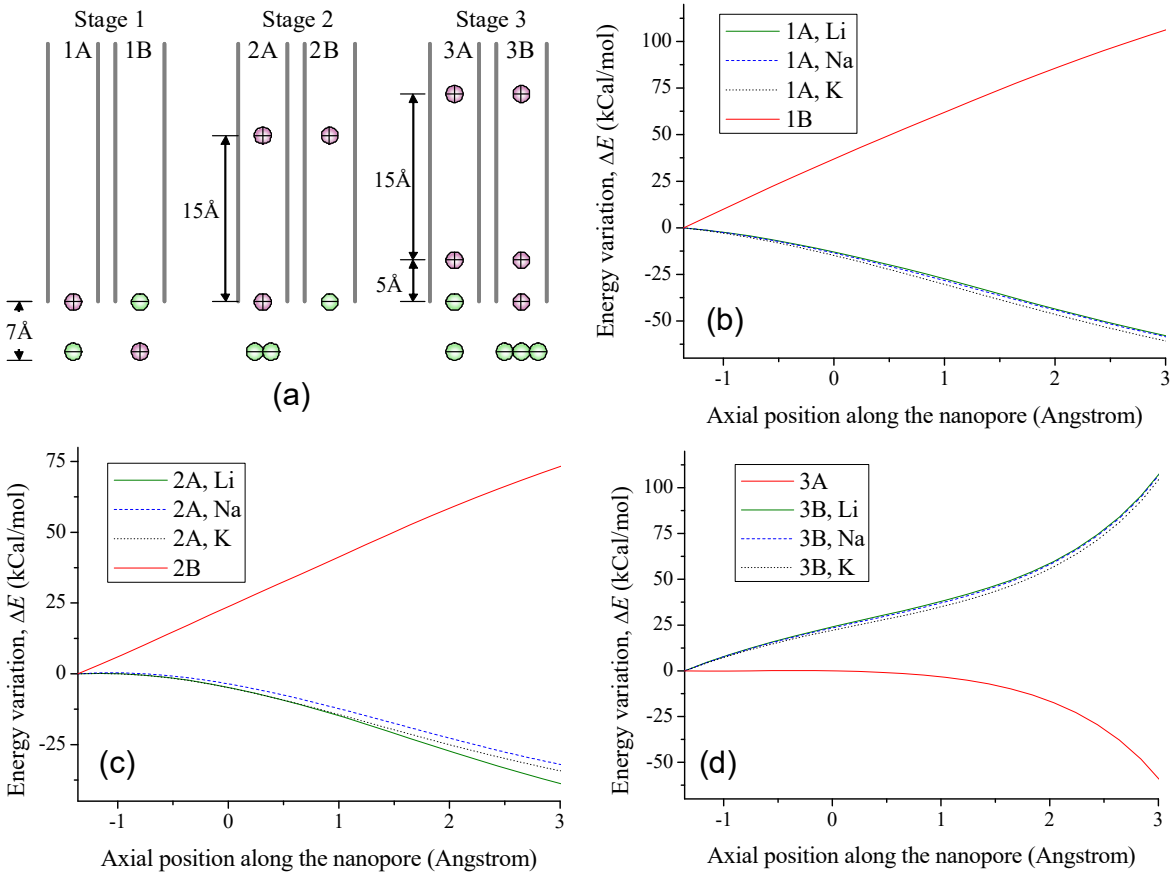
Stage 1
Stage 2
Stage 3
1A
1B
2A
2B
3A
3B
15Å
15Å
5Å
7Å
(a)
1A, Li
1A, Na
1A, K
1B
Energy variation, ΔE (kCal/mol)
(b)
Axial position along the nanopore (Angstrom)
2A, Li
2A, Na
2A, K
2B
(c)
3A
3B, Li
3B, Na
3B, K
(d)

Figure S2

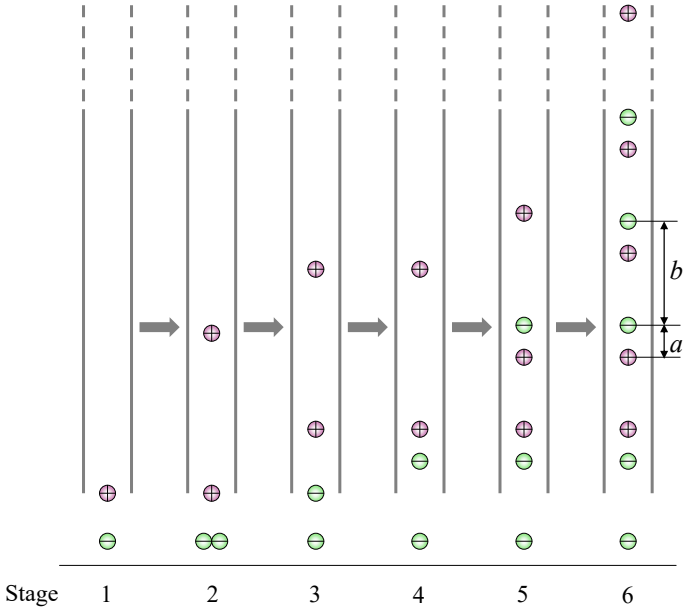

Figure S3

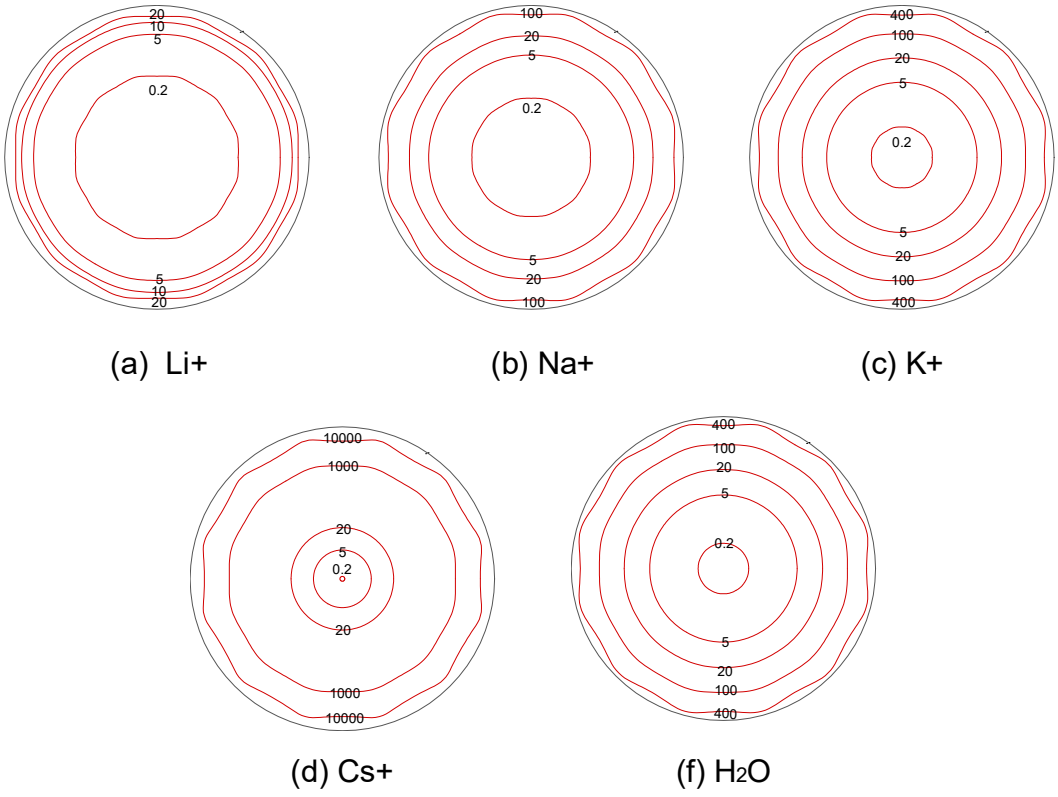
20
10
5
0.2
5
10
20
(a) Li+
100
20
5
0.2
5
20
100
(b) Na+
400
100
20
5
0.2
5
20
100
400
(c) K+
10000
1000
20
5
0.2
20
1000
10000
(d) Cs+
400
100
20
5
0.2
5
20
100
400
(f) H2O

Figure S4

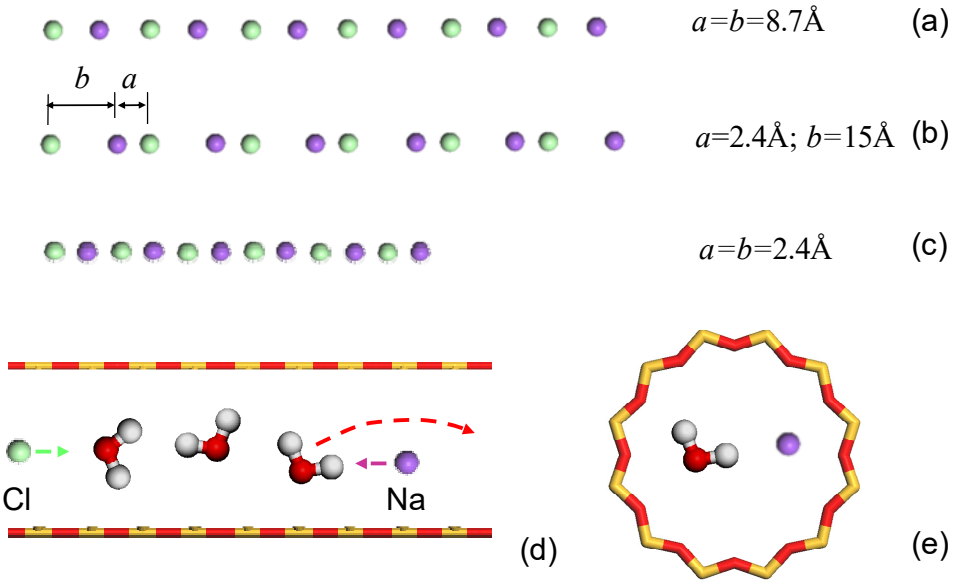

[1] Y. Qiao, L. Liu, and X. Chen, Nano Letters, in press (2009).